Distance and Orientation Measurement of a Flat Surface by a Single Underwater Acoustic Transducer

Vincent Creuze

DISTANCE AND ORIENTATION MEASUREMENT OF A FLAT SURFACE BY A SINGLE UNDERWATER ACOUSTIC TRANSDUCER

Vincent Creuze

LIRMM, CNRS / University Montpellier 2
161 rue Ada, 34095, Montpellier, France
phone: + (33) 467.418.514, fax: + (33) 467.418.500, email: creuze@lirmm.fr
web: www.lirmm.fr

ABSTRACT

In this paper, we detail a new method that allows measuring simultaneously distance and orientation of a flat horizontal or vertical surface (e.g. wall, flat bottom) with a single acoustic transducer. A single mono-frequency ping is necessary. Then the analysis of the peaks in the received echo is sufficient to find out both distance and orientation. This method does not require any a priori knowledge of the target backscattering properties. Its advantages are: a very high sampling rate, the smallest and cheapest sensor, and low acoustic interferences with other acoustic devices (single frequency, short ping). We present theoretical aspect, simulation results, and experiments.

1. INTRODUCTION

Many applications of underwater vehicles (remotely operated or autonomous) require the orientation and distance measurement of a flat surface in order to achieve partially / fully autonomous survey. For instance, video surveys of hydraulic dams by underwater vehicles allow cracks or weaknesses detection. Many interesting sensing approaches have been developed in the literature. Some rely on digital imaging associated with laser triangulation. However, this method suffers from range limitation due to the possible turbidity of the water. Other methods rely on acoustic sensing. Then distance and orientation of the wall are obtained by achieving segmentation of the image acquired by sector scanning sonars [1] [2], or by using directly the beams of a Doppler Velocity Log [3]. These approaches are very well suited to the underwater environment but need expensive and quite big sensors (more than 5k€, and sizing at least 10cm x 6cm²). Other techniques use difference of time-of-flight with two or more transducers, and have been implemented on underwater vehicles as well as on terrestrial vehicles [4]. There also exist techniques based on a single transducer. Some rely on template matching or spectral analysis [5], but require a high computational power. An original single transducer based technique uses the measurement of the time difference of the zero-crossing points of the echo of the surface. It allows accuracy of the order of 1° within a 10° range [6]. The new method that we propose in this paper is based on the directivity pattern of a single transducer and allows orientation detection within a 20° range with the same accuracy. In addition, it requires only a short ping emission at a single frequency. The processing of the received echo allows us to find out both orientation and distance of a flat surface without a priori knowledge of its backscattering properties. In comparison with other acoustic methods, ours offers the following advantages:

- Highest sampling rate (only one ping is required to compute both distance and orientation) and shortest acquisition time (in comparison with sector scanning sonar for instance).
- Single frequency emission thus minimizing interferences with other acoustic devices (e.g. modem).
- Low power consumption, small computational cost.
- The sensor is basic, cheap and small (in comparison with arrays of sensors).
- No rotating part (e.g. rotating antenna).

First, we briefly remind the principles of directivity patterns and underwater sound backscattering. Then, we will detail the method and present an algorithm for automatic computation of the received echo. In the last part, simulation and experimental results will be detailed.
Before being published, this work has led to the filing of the European Patent application n°EP11305048.8, on January 17th 2011, entitled "Method and device for measuring distance and orientation using a single electro-acoustic transducer".

2. PROBLEM STATEMENT

2.1 Problem statement

We consider the situation of an underwater Remotely Operated Vehicle (ROV) aiming to navigate at constant distance and orientation of a vertical wall (Fig. 1). d denotes the distance between the wall and the transducer along the u axis. ψ is the wall's orientation measured between the v axis and the wall. The orientation of the line of sight of the transducer (= axis of the main lobe) regarding the vehicle axis u is denoted γ and is supposed to be constant (mechanically fixed) and known. The transducer is disc-shaped but could be replaced by any other type of transducer as long as its directivity pattern contains at least two lobes. The pitching angle of the ROV is supposed to be null, i.e. the body-fixed axes u and v remain horizontal.

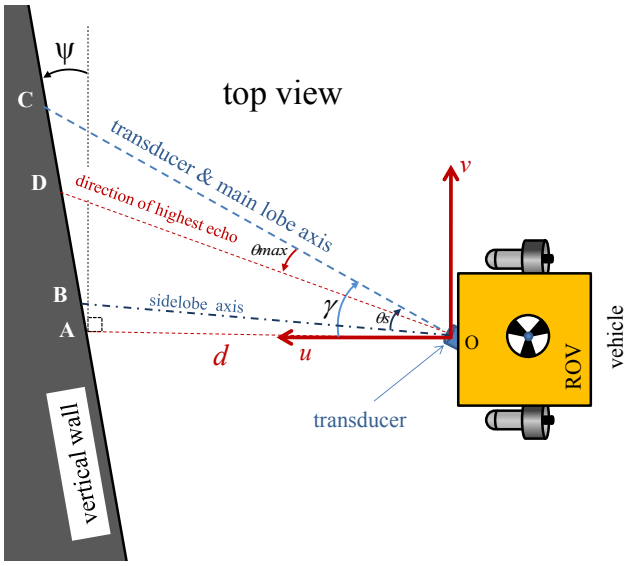

Figure 1 – Top view of the underwater vehicle (ROV) navigating along the vertical wall. The transducer is placed in O. (O,*u*,*v*) is the body-fixed frame of the ROV.

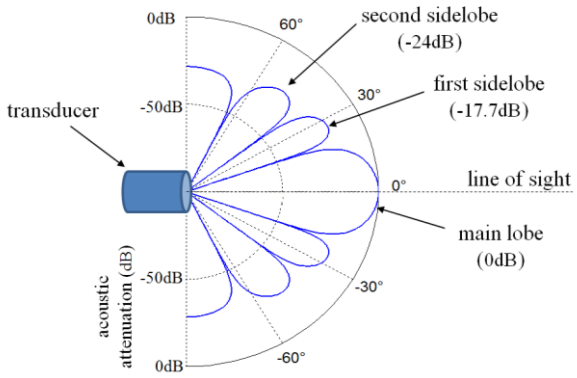

Fig. 2 - Directivity pattern of a disc-shaped transducer (radius=13.5 mm, *f*=200 kHz). The sidelobe attenuation is -17.7dB.

2.2 Directivity pattern and backscattering

It is well-known that the directivity pattern $b(\theta)$ of a disc shaped-transducer is given by:

$$b(\theta) = \left(\frac{2J_1\left(2\pi f \frac{r_c}{c} \sin\theta\right)}{2\pi f \frac{r_c}{c} \sin\theta} \right)^2 \quad (1)$$

where $J_1(.)$ is the first order Bessel function, f is the acoustic wave frequency ($200\ kHz$), r_c is the transducer radius, and c is sound speed in water ($1500\ m.s^{-1}$) [7]. A polar representation of the directivity pattern in decibels highlights the main lobe and the sidelobes (Fig. 2). In the following, "sidelobe" will designate only the first sidelobe (17.7dB attenuation). Others are weak enough to be neglected (their attenuation is larger than 24dB).

The sidelobe has usually no effect because it is very weak and hits the target (e.g. seabed in the case of echo-sounder) with large incidence angles.

The backscattering strength S_s for the surface reverberation of the wall (or of the bottom in the case of bottom tracking) is given in $dB.m^{-2}$ and is defined as the ratio, in decibel units, of the backscattered intensity produced by a unit area of the wall to the incident intensity. For incidence angle φ_i beyond $25°$, a good approximation of the backscattering strength S_S is given by Lambert's law [8]:

$$S_S = S_0 + 10 \log \cos^2 \varphi_i \quad (2)$$

where S_0 is a constant parameter depending on the wall characteristics, and φ_i is the incidence angle.

For incidence angles φ_i less than 25°, the backscattering strength S_S can be approximated by (linear approximation):

$$S_S = S_N + \frac{\varphi_i}{\varphi_0}(S_0 - S_N + 10 \log \cos^2 \varphi_0) \quad (3)$$

where S_N is the backscattering strength for normal incidence and φ_0 is called the transition direction.

2.3 Two lobes, two peaks

If the transducer is tilted, the incidence angle of the main lobe is larger than the one of the sidelobe (Fig. 1). Then, the backscattering strength is lower for the main lobe signal than for the sidelobe. Moreover, due to the difference in length of the sound paths, transmission losses TL (mainly spherical spreading, as the distance is short) are lower for the sidelobe than for the main lobe. Consequently, in spite of directivity attenuation, the global attenuation level H makes the sidelobe echo level significant in comparison with the main lobe echo level. Moreover, as the distance to the wall is smaller for the sidelobe than for the main lobe (Fig. 1), the echo of this latter will be received after the one of the sidelobe. Thus, the backscattered acoustic echo consists of two separated parts corresponding first to the sidelobe and secondly to the main lobe (Fig. 6).

In the following, we will explain how the time of occurrences of the maximum of both echoes can lead to the computation not only of the distance but also of the orientation.

3. PRINCIPLE OF DISTANCE AND ORIENTATION MEASUREMENT

3.1 Intuitive approaches

In order to find out the orientation of the wall, some approaches consist in analyzing the shape of the second part of the echo (template matching). However, the backscattering parameter S_0 is *a priori* unknown. It depends on the reflecting surface (concrete wall, metallic hull, seabed…) and strongly affects the shape of the second part of the echo. Thus, without a good knowledge of S_0, the shape analysis of the second part of the echo will not lead to a precise estimation of the orientation of the wall.

Another approach could be to consider that the maximum of intensity of the first part of the echo corresponds to the axis of the sidelobe, and the second part of the echo corresponds to the axis of the main lobe. Thus, one could easily

recover distance and orientation by simple trigonometric equations. This is wrong. In fact, the echo of sidelobe is so narrow that its maximum could be considered to correspond to its axis, but, due to spherical spreading and backscattering angle dependency, the maximum of intensity of the second part of the echo does not correspond to the axis of the main lobe. In the following, we will explain how to determine in which direction of the beam the maximum of sound echo is received. This is also called the "*highest echo direction*" in Fig. 1.

3.2 Expressing the maximum of the echo as a function of orientation ψ

We propose to study the echo intensity as a function of θ, where θ is an angle difference with the axis of the main lobe (Fig. 1). In the following, ψ is the wall orientation angle and d is the distance between the transducer and the wall along the u axis of the vehicle. The incidence angle in the θ direction is denoted $\varphi_i(\theta)$, and the distance between the transducer and the wall along θ direction is $r(\theta)$.

Thus, we have the following relationships:

$$\varphi_i = \gamma + \theta - \psi \tag{4}$$

and

$$r(\theta) = d\frac{\cos(\psi)}{\cos(\gamma+\theta-\psi)}. \tag{5}$$

Let us now determine $H(\theta, d, \psi)$, the function defining the echo attenuation in θ direction. Absorption will be neglected within transmission losses as its effect is very small in comparison with spherical spreading (the measured distances in this application are less than 15 meters).

Thus, considering the two-way configuration of our transducer, the two-way spherical spreading losses, and the backscattering (angle of incidence of the main lobe is beyond 25° so Lambert's law applies), we have:

$$H(\theta,d,\psi)=\left(\frac{2J_1\left(2\pi f\frac{r_c}{c}\sin\theta\right)}{2\pi f\frac{r_c}{c}\sin\theta}\right)^4 \frac{1}{\left(d\frac{\cos(\psi)}{\cos(\gamma+\theta-\psi)}\right)^4}\, i_{f0}\cos^2(\gamma+\theta-\psi) \tag{6}$$

where $i_{f0} = 10^{S_0/10}$, with S_0 defined in 2.2.

Then, one can see that the derivative $\frac{dH(\theta,d,\psi)}{d\theta}$ neither depends on the distance d, nor on the backscattering parameter S_0, which means that the angle $\boldsymbol{\theta_{max}}$ **corresponding to the maximum of** $\boldsymbol{H(\theta, d, \psi)}$ **depends only on** $\boldsymbol{\psi}$ (other parameters f, r_c, c, and γ are known constant values). Thus θ_{max} can be expressed as $\theta_{max} = g(\psi)$, where g is a nonlinear function. Of course, $\frac{dH(\theta,d,\psi)}{d\theta} = 0$ has no simple analytical solution, thus g cannot be expressed analytically. However, it is very easy to numerically compute g and interpolate it by a second order polynomial called $\hat{g}$ (Fig.3). As it depends only on the measured directivity pattern (it does not depend on d or S_0), $\hat{g}$ has to be computed only one time (off-line). Once we know $\hat{g}$, it becomes easy to estimate the wall orientation.

The use of the interpolation $\hat{g}$ instead of g will allow easier implementation (on DSP) of the algorithm described in the following.

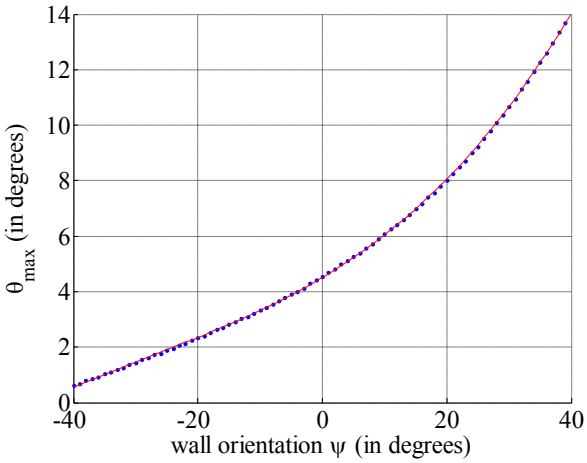

Figure 3 – With the following set of parameters ($\boldsymbol{f = 200\,kHz}$, $\boldsymbol{r_c = 1cm}$, $\boldsymbol{c = 1500\,m.s^{-1}}$, $\boldsymbol{\gamma = -47.8°}$), function $\boldsymbol{\theta_{max} = g(\psi)}$ (blue dots) can be interpolated (solid red line) by $\boldsymbol{\hat{g}(\psi) = 0.0017\psi^2 + 0.134\psi + 4.506}$

It has also to be noticed that the assumption of Lambert's law incidence of the main lobe is true only if the orientation of the wall with respect to the v axis of the ROV is greater than -10° (this mainly depends on the aperture of the main lobe and on the γ angle). As orientation and distance of the ROV with respect to the wall is close-loop controlled, ψ can be assumed to be maintained close to 0°. Initialisation of this process is out of the scope of this paper, but one can briefly say that this is achieved by a 360° rotation of the ROV. In fact, when ψ is out of the range [-10° +10°], there is either only one echo (superimposition) or no echo (sound is not emitted in the wall direction).

3.3 Orientation and distance

Angles shown on fig. 1 can be expressed as follows:

$$\widehat{ABO} = \frac{\pi}{2} - \psi + \gamma - \theta_s \tag{7}$$

$$\widehat{ADO} = \frac{\pi}{2} - \psi + \gamma + \theta_{max} \tag{8}$$

$$\widehat{OAD} = \frac{\pi}{2} + \psi \tag{9}$$

where θ_s is the angle between the axis of the sidelobe and the axis of the main lobe (obtained from the directivity pattern of the transducer).

Then, we have the following equations:

$$\frac{d}{\sin\widehat{ABO}} = \frac{c.t_s/2}{\sin\widehat{OAD}} \tag{10}$$

$$\frac{d}{\sin\widehat{ADO}} = \frac{c.t_m/2}{\sin\widehat{OAD}} \tag{11}$$

where t_s and t_m are respectively the times of occurrence of the maxima of the two parts of the received echo (Fig. 4).

As c denotes the sound speed, $c.t/2$ denotes the distance between the source and an impact point.

Equations (10) and (11) lead to:

$$t_s \cos(\psi - \gamma + \theta_s) - t_m \cos(\gamma - \psi + \theta_{max}) = 0 \quad (12)$$

Replacing θ_{max} by $\hat{g}(\psi)$ in (12) gives us the equation to solve to find out ψ.

$$t_s \cos(\psi - \gamma + \theta_s) - t_m \cos\left(\gamma - \psi + \hat{g}(\psi)\right) = 0 \quad (13)$$

Although there is no analytical solution, equation (13) can be easily numerically solved. Once orientation ψ has been determined, the distance d is computed by applying (10) or (11).

3.4 Ping duration

The duration of the acoustic ping to be emitted depends on the distance d. The closer from the surface we are, the shorter must be the ping in order to keep the ability to distinguish both peaks. In fact the shape of the peaks t_s and t_m depends on the ping duration, and a too long ping would lead to superimposed echoes of both lobes.

4. AUTOMATIC SIGNAL PROCESSING

Automatic processing of the received acoustic echo can be implemented by the following algorithm:

Step 1 Low-pass filtering of the echo to extract the envelope of the echo.

Step 2 Detecting the summits locations t_s and t_m, for instance by computing the first derivative of the echo envelope.

Step 3 Numerically solving (13), for instance by computing all the values of the left part of the equation starting from ψ_{min} (the smallest detectable value within the angular range of this system) until its sign changes (of course more efficient methods can be applied depending of the computing capabilities of the chosen device).

Step 4 Once orientation ψ has been computed, it is easy to compute the distance d by using (10) or (11).

5. SIMULATION RESULTS

5.1 Simulation environment

Simulations have been conducted with Matlab™ environment. The reflecting surface is meshed. Each cell of the grid is far smaller than the product $c.\tau$, where τ is the ping duration and c is the sound speed. All the contributions of the mesh are weighted (depending on their attenuation), time delayed (depending on their position) and then added to compute the received echo.

Comparison of the simulation results with experimental acquisitions shows the ability of the simulator to reproduce the echo shape.

As the echo intensity strongly depends on both sensor and environmental parameters, the echo intensity plotted on simulations has no unit (they should be in Pa or dB). In fact, on the following plots, the intensity scale is relative and should be multiplied by an appropriate constant to get the true intensity. As we only focus on the shape of the echo and the arrival time of its peaks, the depicted intensity will be only relative.

5.2 Simulation results

Simulations have shown that ψ can be properly estimated within the range [-10° +10°]. Depending of backscattering properties of the reflecting surface and depending on the directivity pattern of the transducer, this latter range value could be extended. However for autonomous navigation purposes, the vehicle orientation has to be kept constant (with respect to the tracked surface). Once the sensor is well oriented, the measurement range of our system is sufficient for servoing the vehicle position. If a wider measurement range is necessary, the transducer could be actuated by a servomotor.

Figure 4 shows simulation results with the following set of parameters: f=200 kHz, $r_c = 1\text{cm}$, $c = 1500\ m.s^{-1}$, $\gamma = -37.8°$, $d = 10m$, $\psi = +10°$ (first plot) or $\psi = 0°$ (second plot). One can see the simulated received echo (in blue solid line) and the times of arrival of the two maxima (in red). Applying the automatic signal processing algorithm described in §4 leads to the following results: $d = 9.94m$, $\psi = +9.9°$ (first plot) and $d = 10.08m$, $\psi = 9.7°$ (second plot).

For values smaller than -10°, echoes of the two lobes occur too closely or are superimposed (Fig. 5).

For values bigger than +10°, the intensity of the sidelobe echo decreases and it becomes harder to detect its maximum.

The errors measured during simulations (within the range -10° +10°) are the following: distance error < 2%, orientation error < 1°.

6. EXPERIMENTS

We are currently conducting experiments of the system (pool tests). First results confirm the simulation results but the number of experiments is not yet sufficient to give a precise experimental estimate of the measurement errors. Figure 6 shows an acoustic acquisition made under the following conditions: $d = 2.2m$, $\psi = +5°$. The values obtained by computing the time of arrival of the two peaks are $d = 2.18m$, and $\psi = +4.9°$.

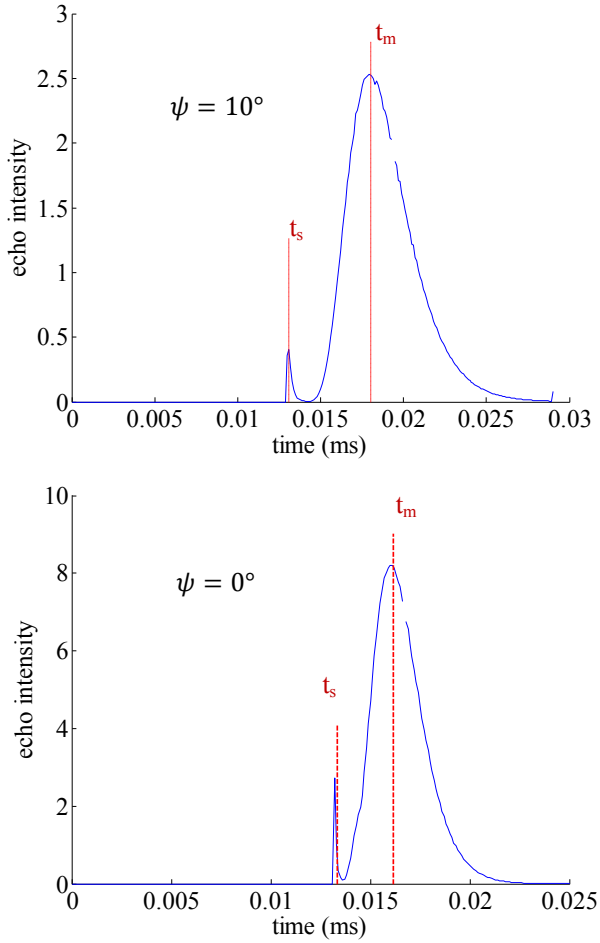

Figure 4 – Simulations of acoustic echos (f=200 kHz, r_c = 1cm, $c = 1500\ m.s^{-1}$, $\gamma = -37.8°$, $d = 10m$, $\psi = 10°$ *or* 0°). The first small peak corresponds to the echo of the sidelobe, while the second peak corresponds to the echo of the main lobe.

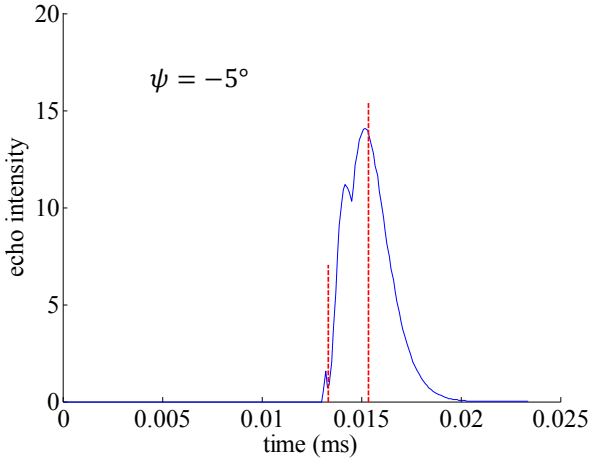

Figure 5 – Simulation of an acoustic echo outside the range (f=200 kHz, r_c = 1cm, $c = 1500\ m.s^{-1}$, $\gamma = -37.8°$, $d = 10m$, $\psi = -5°$). Both peaks are superimposed and thus cannot be distinguished.

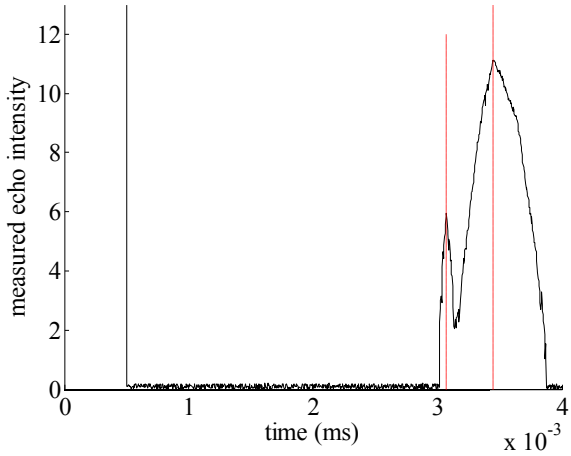

Figure 6 – Experimental acquisition of an acoustic echo (in a pool). Peaks can easily be detected and lead to an appropriate estimate of distance and orientation of the bottom of the pool.

7. CONCLUSION

More experiments will be conducted in the next months in order to verify the experimental accuracy of the system. This work has been presented for the 2D geometry of a vertical wall. The case of non vertical surfaces (3D) is under study. However, as the above-described principles also apply in the air, many applications exist for terrestrial (e.g. wall following) or aerial robotics (floor or ceiling following).

REFERENCES

[1] Y. Petillot, I. Tena Ruiz, and D. M. Lane, "Underwater Vehicle Obstacle Avoidance Using a Multi-Beam Forward Looking Sonar," *IEEE Journal of Oceanic Engineering*, Vol. 26, no. 2, pp. 240-251, April 2001.

[2] J.J. Leonard and H.F. Durrant-Whyte, "Directed Sonar Sensing for Mobile Robot Navigation," *ser. The Kluwer International Series in Engineering and Computer Science*, Norwell, MA: Kluwer, 1992.

[3] R. Damus, S. Desset, J. Morash, V. Polidoro, F. Hover, C. Chryssostomidis, J. Vaganay and S. Willcox, "A new paradigm for ship hull inspection using a holonomic hover-capable AUV," *Informatics in control, automation and robotics I*, Springer Netherlands, 3, pp. 195-200, 2006.

[4] T. Yata, A. Ohya, S. Yuta, "A fast and accurate sonar ring sensor for a mobile robot," *in Proc. IEEE Int. Conf. Robot. Autom.*, pp. 630–636, 1999.

[5] T. Yata, S. Yuta, "Measurement of reflecting direction from the center frequency of the echo in ultrasonic sensing," Advanced Robotics: International Journal of Robotics Society of Japan, Vol. 11, n°3, pp 269-283, 1997.

[6] T. Yata, L. Kleeman, and S. Yuta , "Wall Following Using Angle Information Measured by a Single Ultrasonic Transducer," *in Proc. of the 1998 IEEE International Conference on Robotics and Automation*, pp. 1590-1596, 1998.

[7] R.J.Urick, *Principles of Underwater Sound*, Peninsula Pub, 1996.

[8] X. Lurton, *An introduction to Underwater Acoustics – Principles and Applications*, Springer Praxis Books, 2003.